Mitigating Misaligned Hall Sensors in Brushless DC Motors Using a Calibration Routine for Improved Fast Electromechanical Transients

by

Matthew Hasman

BASc., The University of British Columbia, 2025

A THESIS SUBMITTED IN PARTIAL FULFILLMENT OF

THE REQUIREMENTS FOR THE DEGREE OF

BACHELOR OF APPLIED SCIENCE

in

THE FACULTY OF APPLIED SCIENCE

(ELECTRICAL AND COMPUTER ENGINEERING)

THE UNIVERSITY OF BRITISH COLUMBIA

(Vancouver)

April 2025

The following individuals certify that they have read, and recommend to the Faculty of Graduate and Postdoctoral Studies for acceptance, the thesis entitled:

Mitigating Misaligned Hall Sensors in Brushless DC Motors Using a Calibration Routine for Improved Fast Electromechanical Transients

submitted by Matthew Hasman in partial fulfilment of the requirements for

the degree of Bachelor of Applied Science

in Engineering Physics

Examining Committee:

Dr. Juri Jatskevich, Electrical and Computer Engineering
Supervisor

Abstract

Hall-sensor-controlled brushless DC (BLDC) motors are commonly used in many applications due to their low cost and simple control. In a typical BLDC motor, a permanent magnet synchronous machine (PMSM) is controlled by a voltage source inverter (VSI) using the Hall sensor signals. Ideally, the three Hall sensors are spaced 120 electrical degrees apart. However, due to manufacturing tolerances, the sensors' actual position may differ, resulting in uneven conduction intervals and degradation of motor performance. Previous research proposed averaging the Hall sensor signals to mitigate the misaligned Hall sensors and achieve a steady state performance close to ideal. However, such averaging filters have a memory and may degrade the dynamic performance in fast transients. To enable fast dynamic performance, this thesis proposes a calibration routine that identifies the errors and records the necessary correction values in a lookup table. The stored correction angles from the lookup table are then applied to the Hall sensor signals at run time, which removes the delay present in the averaging filter method and significantly improves the dynamic performance of the BLDC motors during fast electromechanical transients.

Lay Summary

Hall-sensor-controlled brushless DC (BLDC) motors are commonly used in many applications due to their low cost and simple control. Ideally, the three Hall sensors are spaced 120 electrical degrees apart. However, due to manufacturing tolerances, the sensors' actual position may differ, resulting in degradation of motor performance. This thesis proposes a novel method based on a calibration routine that identifies the errors and records the necessary correction values in a lookup table. The stored correction angles from the lookup table are then applied to the Hall sensor signals at run time, which removes the errors and significantly improves the dynamic performance of the BLDC motors during fast electromechanical transients. It is envisioned that the proposed method may become widely adopted in applications that use BLDC motors, improving their quality and cost-effectiveness.

Preface

This thesis represents a continuation of the line of research carried out at the UBC's EPES research group and makes additional original contributions. In preparing this thesis, I was the primary author responsible for most of the work, including deriving model equations, building the simulation models, implementing correction algorithms, conducting and processing experiments, and writing and editing initial drafts. My supervisor, Dr. Juri Jatskevich, provided valuable guidance throughout the entire research process, providing directions and helping me improve results. My friend and partner, Mark Phung, provided valuable help in implementing our ideas and providing constructive feedback on initial drafts. Ziliang Feng, a MASc student with the EPES research group, provided us with support through this research project, helping us learn the theory and conduct the hardware experiments. In accordance with the IEEE PSPB Publication Manual - Authorship, these people are included as co-authors in my publications. It should be stated that:

Chapter 2 is based on the following conference paper that has been published:

> **M. Hasman,** M. Phung, Z. Feng and J. Jatskevich, "Mitigating Misaligned Hall-Sensors in Brushless DC Motors Using Calibration Routine," *IEEE 24th International Symposium INFOTEH-JAHORINA (INFOTEH)*, East Sarajevo, Bosnia and Herzegovina, March 19 – 21, 2025, pp. 1-6, doi: 10.1109/INFOTEH64129.2025.10959174.

Chapter 3 is based on a conference paper that will be submitted:

> **M. Hasman,** M. Phung, Z. Feng and J. Jatskevich, "Microcontroller Implementation of Lookup-Table-based Hall Sensor Correction for Improving Dynamic Performance Brushless DC Motors," *IEEE 7th Global Power, Energy and Communication Conference (GPECOM 2025),* June 11 – 13, 2025, Bochum, Germany, 6 pages.

Table of Contents

List of Tables

List of Figures

List of Symbols

H_1, H_2, H_3	Hall sensor
h_1, h_2, h_3	Hall sensor signal
i_{as}, i_{bs}, i_{cs}	Stator phase current
J	Moment of inertia
$\lambda_{as}, \lambda_{bs}, \lambda_{cs}$	Stator flux linkage
λ'_m	Rotor permanent magnet flux linkage
L_{ls}	Stator leakage inductance
L_m	Stator magnetizing inductance
n	Machine speed
ω_r	Rotor electrical speed
P	Number of poles
ϕ_v	Advance in firing angle
r_s	Stator resistance
t	Time
T_e	Electromagnetic torque

θ_r	Rotor electrical position
T_m	Mechanical load torque
v_{as}, v_{bs}, v_{cs}	Stator phase voltage
V_{dc}	Fixed dc voltage

List of Abbreviations

Abbreviation	Meaning
BLDC	Brushless Direct Current
DC	Direct Current
DSP	Digital Signal Processor
EMF	Electromotive Force
LUT	Lookup Table
MTPA	Maximum Torque per Ampere
MTPV	Maximum Torque per Voltage
PM	Permanent Magnet
PMSM	Permanent Magnet Synchronous Machine
PWM	Pulse-width Modulation
VSI	Voltage Source Inverter

Acknowledgements

I am immensely grateful to my undergraduate thesis supervisor, Dr. Juri Jatskevich, for his incredible support this past academic year, 2024-2025. One year ago, I took the course *ELEC 343 Electromechanics*, offered by Dr. Jatskevich's group. After experiencing the course, I was motivated to pursue further research on electromechanics and motor control. Dr. Jatskevich welcomed me into the Electric Power and Energy Systems (EPES) research group and provided incredible guidance throughout the year to further learn the fundamentals of energy systems and motor control, allowing me to write my undergraduate thesis on this topic. Dr. Jatskevich's invaluable guidance throughout the year made this thesis possible, and he taught me a lot about brushless DC machines and academic writing.

In addition, I would like to thank Mark Phung for his incredible support throughout the year. Mark and I were undergraduate students in Engineering Physics and have worked very closely together this past academic year on our research projects and theses related to brushless DC motors. I learned a tremendous amount working with Mark; he is incredibly knowledgeable about motors and has experience in the design and industry. I would also like to express my gratitude to other members of the EPES research group, particularly Ziliang (Bruce) Feng, who supported us in nearly every stage of this process, helping us perform experiments and better understand the theory required to make the progress that we all have achieved.

To my beloved Mom and Dad

Chapter 1: Introduction

1.1 Background

Brushless DC (BLDC) motors are commonly used in industrial automation and other electromechanical applications. Hall-sensor-controlled BLDC machines are widely chosen due to their simplicity, low cost, and ability to operate at a wide range of speeds [1]-[4], as well as applications where sensorless control may not be preferred. A BLDC motor consists of a permanent magnet synchronous machine (PMSM), which is electronically commutated by a voltage source inverter (VSI). A schematic diagram of a typical BLDC motor drive is shown in Fig. 1-1, where the VSI is controlled using three Hall sensors that detect the rotor position.

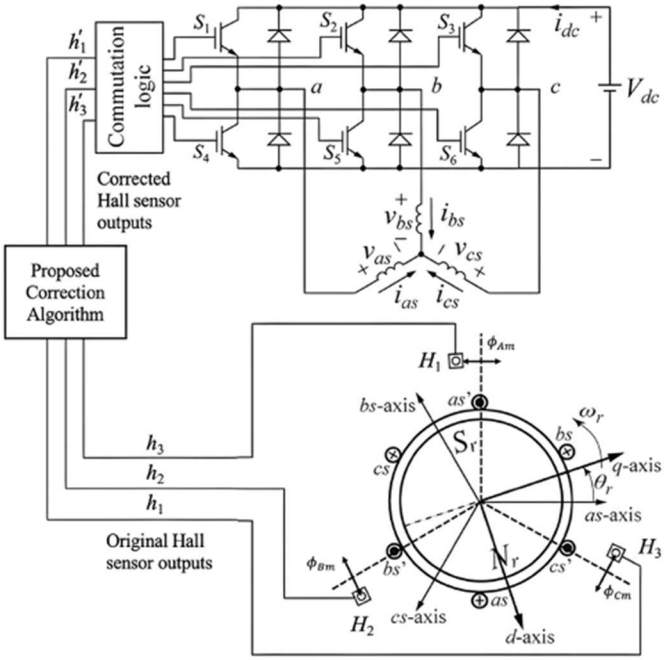

Figure 1-1 A system-level diagram for a Hall-sensor-controlled BLDC motor driven by a voltage-source-inverter [6]. The Hall sensors are misaligned, and Hall signals are passed through the proposed correction algorithm.

Each Hall sensor outputs a square wave signal with a value of 1 or 0, depending on the rotor position. To provide six evenly spaced readings of the rotor position, the three Hall sensors must be spaced apart by 120° [5]. Generally, a BLDC motor can be controlled with either a 180° or 120°-commutation scheme [8]. For the 180°-commutation scheme, each phase conducts for 180 electrical degrees. In contrast, for the 120°-commutation scheme, each phase conducts for 120 electrical degrees and then floats for 60 degrees two times within the electrical cycle. This commutation scheme is more common because it forces the fundamental component of the phase current to be approximately aligned with the corresponding phase back electromotive force (EMF). An advance/delay in firing angle, denoted in Fig. 1-1 by angle, may be applied by shifting the Hall sensors (either mechanically or digitally, using code inside the microcontroller) to switch the inverter transistors earlier or later, and thus implement some specific control schemes such as maximum torque per voltage or maximum torque per Ampere [8].

Notably, the placement of Hall sensors is subject to inaccuracy due to manufacturing tolerances, and low-precision BLDC motors can have significant offsets in sensor placement [6], [7]. An example of a typical industrial BLDC motor and its Hall sensor PCB assembly is shown in Fig. 1-2, where the Hall-sensor misalignment is also illustrated. Such errors in Hall sensor placement generally lead to uneven commutation intervals, increased current and torque ripple, audible noise or mechanical vibrations, and degradation of motor performance [9]. Therefore, mitigating the impact of inaccurate Hall sensors may enable less expensive BLDC motors to be viable in applications requiring higher precision.

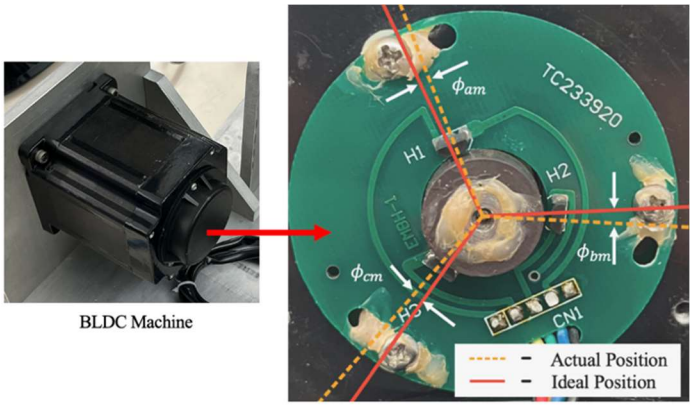

Figure 1-2 Typical brushless DC motor and its Hall sensors: (a) motor case and mount, and (b) a printed circuit board with Hall sensors H_1, H_2, and H_3, which are visibly misaligned.

1.2 Motivation and Research Objectives

To improve performance caused by misaligned Hall sensors, many investigations have been conducted, e.g. [6], [10], [11] exploring different mitigation techniques. In particular, average-type filtering techniques [10] have successfully balanced the Hall signals and removed uneven commutation in steady-state operation. However, averaging filters pose several drawbacks, including increased delay and poor performance during fast transients [9].

Therefore, this thesis makes a contribution and proposes a new solution that achieves correction accuracy similar to the average filtering approach but without unwanted delay. The proposed correction algorithm, shown in Fig. 1-1 as a block that processes the Hall sensor signals, has two modes: i) calibration stage, where the errors are identified and recorded into a lookup table (LUT); and ii) restored operation using the necessary corrections from the LUT at run time without any delays. The calibration mode uses filtering techniques to correct sensor misalignment and then learns correction angles. The corrected operation using the LUT re-computes the saved angle errors into appropriate timing corrections for properly switching the VSI transistors. The algorithm does not require extensive computation and may be carried out on existing/low-cost

microcontrollers. The proposed correction algorithm does not require additional hardware and can thus be added to most BLDC motor controllers without incurring extra costs.

1.2.1 Objective I: Model the BLDC machine with Hall-sensor misalignment and then apply a correction algorithm in the simulation

Previous research on BLDC machines used filtering schemes to balance Hall signals. These filtering techniques successfully balance signals; however, they lead to unwanted delay, leading to performance degradation during transient behaviour. The first objective is to achieve a simulation of a BLDC machine to implement a new correction algorithm to balance Hall signals without adding unwanted delay. The algorithm can be refined and validated on various machine parameters by testing the proposed calibration routine in simulation before being introduced to a microprocessor.

1.2.2 Objective II: Present a microprocessor implementation of the control algorithm on a typical BLDC machine and present measurement results

After testing the proposed algorithm extensively in simulation, the second goal is to implement the new method on a standard BLDC machine with a commonly used microprocessor. The second objective showcases measurement data for the algorithm implemented on real hardware to show the improvement of dynamic performance when using the proposed correction method.

Chapter 2: Simulation Study for a BLDC Machine with Misaligned Hall-Sensors

2.1 Modelling a Hall-sensor-controlled BLDC Machine

2.1.1 Electrical dynamics

The BLDC motor is assumed to use a PMSM with VSI commutation. The electrical dynamics of a three-phase PMSM are commonly expressed in phase variables in the form of the voltage equation [12], [13]

$$\mathbf{v}_{abcs} = \mathbf{r}_s \mathbf{i}_{abcs} + \frac{d\boldsymbol{\lambda}_{abcs}}{dt}, \tag{2.1}$$

where $\mathbf{v}_{abcs}$ denotes the vector of phase voltages, $\mathbf{i}_{abcs}$ denotes the vector of phase currents, $\mathbf{r}_s$ represents the stator resistance matrix, and $\boldsymbol{\lambda}_{abcs}$ is the flux linkage vector. The flux linkage $\boldsymbol{\lambda}_{abcs}$ is a combination of components contributed by the permanent magnet and the phase currents, and it can be described as

$$\boldsymbol{\lambda}_{abcs} = \mathbf{L}_s \mathbf{i}_{abcs} + \lambda_m \begin{pmatrix} \sin(\theta_r) \\ \sin(\theta_r - 2\pi/3) \\ \sin(\theta_r + 2\pi/3) \end{pmatrix}. \tag{2.2}$$

Here, the permanent magnet strength is denoted by λ_m. According to (2), the total flux linkage for each phase is dependent on all stator currents and the rotor position denoted by θ_r. The inductance matrix $\mathbf{L}_s$ is expressed as

$$\mathbf{L}_s = \begin{pmatrix} L_{ls} + L_{ms} & -0.5L_{ms} & -0.5L_{ms} \\ -0.5L_{ms} & L_{ls} + L_{ms} & -0.5L_{ms} \\ -0.5L_{ms} & -0.5L_{ms} & L_{ls} + L_{ms} \end{pmatrix}, \tag{2.3}$$

where L_{ls} is the per-phase stator leakage inductance, and L_{ms} is the magnetizing inductance of each phase.

2.1.2 Mechanical dynamics

For the purpose of this thesis, the mechanical subsystem of the BLDC motor drive is modelled as a single-mass rigid body system described as

$$J_{total}\frac{d\omega_{rm}}{dt} = T_e - T_{fric} - T_m, \tag{2.4}$$

where J_{total} is the total moment of inertia of the machine and the mechanical load, ω_{rm} is the rotor angular mechanical speed, T_e is the developed electromagnetic torque, and T_{fric} are the frictional and T_m mechanical torques respectively.

2.1.3. Hall sensors misalignment

To model Hall-effect sensor misalignment, we denote the mechanical angle of misalignment for each of the sensors ϕ_{Am}, ϕ_{Bm} and ϕ_{Cm} for Hall sensors H_1, H_2, and H_3, respectively. A typical industrial BLDC motor considered in this paper is shown in Fig. 2-1, and its Hall sensor assembly is also shown in Fig. 2-1 (b), where the misalignment angles are made visible for better clarity. For machines with many magnetic poles, the mechanical errors of Hall sensors become magnified, leading to a more significant error in electrical degrees. The error in electrical degrees is expressed as [6]

$$\phi_x = \frac{P}{2}\phi_{xm} \tag{2.5}$$

where the subscript *x* denotes the phases A, B, and C, respectively.

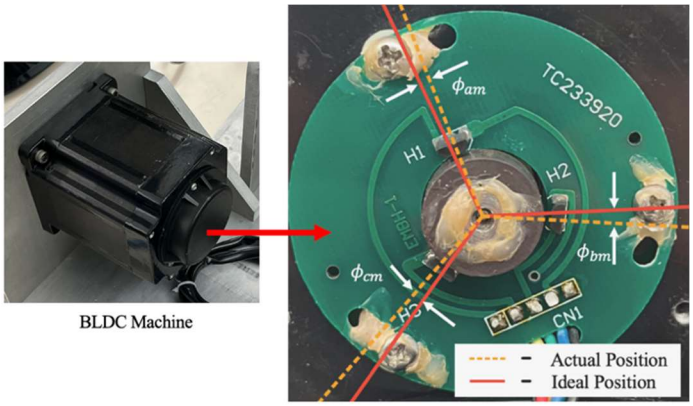

Figure 2-1 Typical brushless DC motor and its Hall sensors: (a) motor case and mount, and (b) a printed circuit board with Hall sensors H_1, H_2, and H_3, which are visibly misaligned.

These errors in sensor positioning are then translated into the corresponding shifts in the Hall sensor signals, as illustrated in Fig. 2-2. For the purpose of modelling, the corresponding errors in the angles have to be considered in the detailed switching model that implements the operation of the VSI transistors.

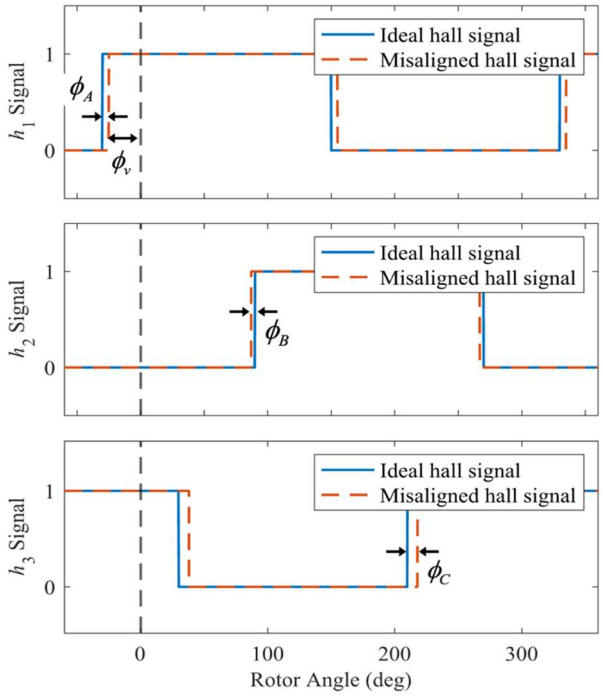

Figure 2-2 Ideal and misaligned Hall-sensor signals.

2.2 Model Verification

A detailed switching model of the subject BLDC motor drive system has been implemented in MATLAB/Simulink using the Simscape Electrical toolbox to verify the proposed methodology. The Hall sensor misalignment errors have been carefully measured on three similar typical industrial BLDC motors in our laboratory. The experimental setup used for the studies is shown in Fig. 2-3. The measured errors are summarized in Table 2-1. As it is observed, the errors may be noticeable, especially when translated from mechanical to electrical degrees. Without loss of generality, Motor 1 was chosen for further studies and investigation presented in this paper. The rest of the motor parameters are summarized in the Appendix.

Table 2-1 Hall-sensor misalignment for three typical BLDC motors available in the lab. Measurements for Motor 1 are used for studies presented in this paper.

Motor Number	ϕ_A	ϕ_B	ϕ_C
1	9.0°	-1.0°	7.0°
2	5.0°	0.5°	-6.5°
3	2.0°	-3.5°	8.0°

To verify the developed Simulink model against the actual hardware setup in Fig. 2-3. The BLDC machine is controlled with a VSI and is attached to a dynamometer load. The motor phase currents were captured and presented in Fig. 2-4. As clearly seen in Fig. 2-4, the three phases are distorted and different among the phases due to the Hall sensor misalignment, leading to fluctuations visible in both the simulated and measured results. It is also seen that using the actual errors of the Hall sensors in the detailed switching model reproduces the motor phase currents in Fig. 2-4 (b) with good accuracy and agreement with the measurements in Fig. 2-4 (a) taken from the subject motor.

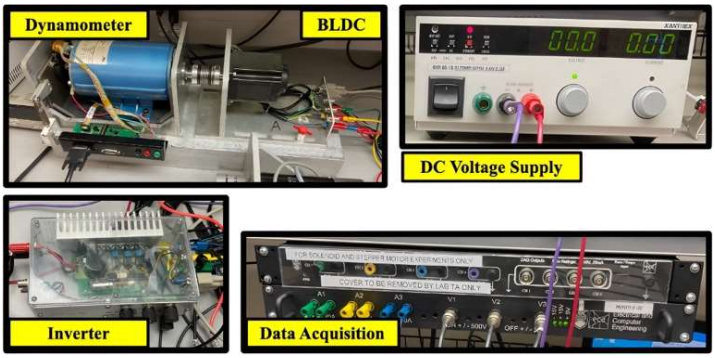

Figure 2-3 Experimental setup for measurements of the subject BLDC motor drive.

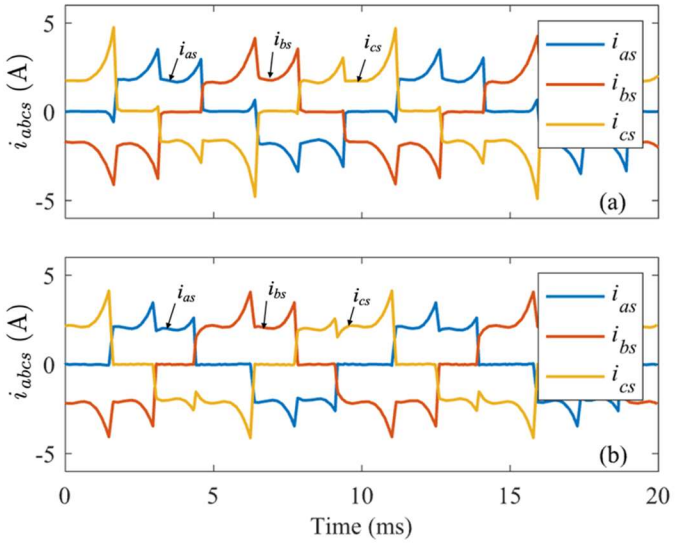

Figure 2-4 The phase current of the subject BLDC motor with misaligned Hall sensors operating in steady state at 24V at 1660rpm: (a) measured phase currents, and (b) simulated phase currents.

2.3 Proposed Methodology

Previous work addressing Hall sensor misalignment in [10] used averaging-type filters to balance the Hall signals. The original Hall sensor signals, denoted by h_1, h_2, and h_3, are inputted into this filter, and then, the filter outputs corrected/balanced signals, denoted by h_1', h_2', and h_3', respectively [10]. To set the stage for the proposed method, let $\tau(n)$ represent the n^{th} conduction interval. Fig. 2-5 illustrates the unbalanced phase currents due to misaligned Hall

sensors, and the time sequence of the corresponding conduction intervals is also labeled as the time-series $\tau(n)$. As seen in Fig. 2-5, the intervals $\tau(n)$ are also fluctuating in duration. The basic idea is to apply the averaging filters to remove the unwanted fluctuations from this discrete-time series of $\tau(n)$.

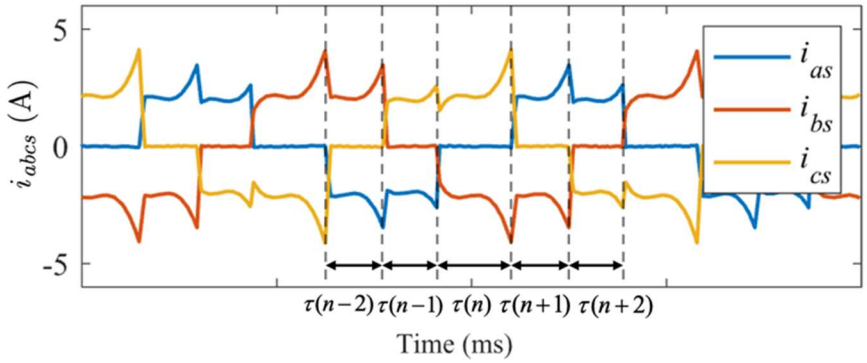

Figure 2-5 Unbalanced switching intervals caused by misaligned Hall sensors.

For the digital implementation of this methodology, the controller reads the time instance of the actual incoming Hall sensor signal (hardware interrupt) and adds a correction time for the next switching instance so that the balancing is enforced. This next switching time instance can be expressed as follows

$$t_{out}(n+1) = t_{in}(n) + \tau^{corr}(n) \tag{2.6}$$

where $t_{in}(n)$ is the time instance the actual Hall sensors switched to its state, and $\tau^{corr}(n)$ is the correction time determined by the filter, and $t_{out}(n+1)$ is the next time that the Hall state should change its state (which will be scheduled by the software interrupt to implement the actual switching of the VSI transistors).

Several such averaging filters have been proposed in [10], including three and six-step filters and extrapolating filters. Omitting the equations of the filters, the following equations are the correction terms of the three and six-step averaging filters, respectively [10]:

$$\tau_{a3}^{corr}(n)=\frac{1}{3}\left(\tau(n-2)+2\tau(n-3)\right) \tag{2.7}$$

$$\tau_{a6}^{corr}(n)=\frac{1}{3}\begin{pmatrix}-\tau(n-1)+\tau(n-3)+\tau(n-4)\\+\tau(n-5)+\tau(n-6)\end{pmatrix}. \tag{2.8}$$

These filters have been shown to balance the Hall-sensor errors successfully in simulation and experimentally. Fig. 2-6 presents the simulation results of applying the 6-step averaging filter in a steady state. As seen in Fig. 2-6, the filter works well, and the conduction intervals become even when the filter is applied. However, the drawback is that any such averaging filter has a memory, which results in a delay and compromises the transient performance induced by the filter [9].

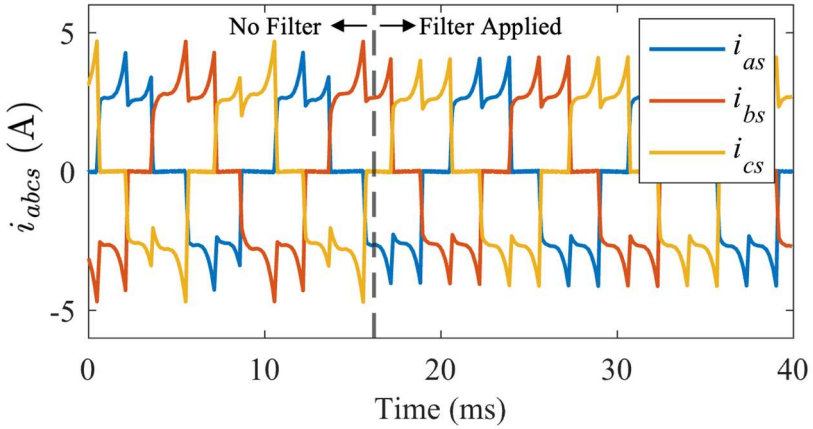

Figure 2-6 Motor phase current when applying either a 6-step averaging filter or a proposed lookup table correction method. Both methods resulted in identical balancing of conduction intervals in a steady state.

The method proposed in this paper extends the previous work by mitigating the impact of the filter delay using a two-stage approach that can be readily implemented on a microcontroller. The control diagram of the proposed correction algorithm is shown in Fig. 2-7. The first is a calibration stage, where the motor reaches a steady state without modifying Hall signals. Then, in a learning

steady state, the errors are corrected using the averaging filter. The observed angle errors are also tabulated and recorded into a lookup table (LUT). In the second stage, the motor uses the LUT to read the corresponding angle corrections and re-calculate the appropriate time corrections used in (6) for restoring the operation. Thereafter, the BLDC motor may be used without using the averaging filter for as long as the values stored in the LUT remain valid, which removes the delay introduced by the averaging filter. The operating modes of this method are described in more detail below.

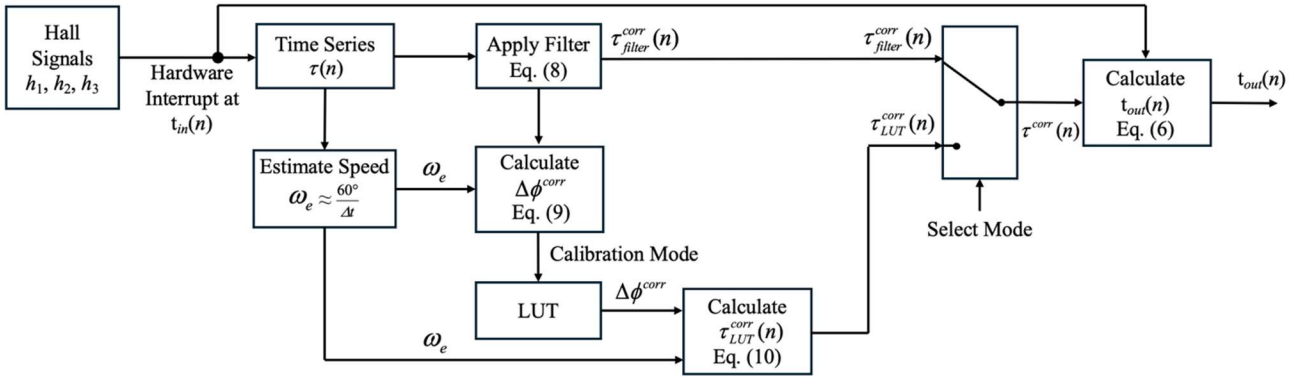

Figure 2-7 The control flow diagram for the proposed correction algorithm. Initially, during calibration, the system applies a filter to balance Hall signals and stores the correction angles into a LUT. Afterwards, the controller uses previously stored correction angles to restore the Hall signals without using a filter.

2.3.1. Calibration mode

During calibration, the motor first reaches a steady state operation. Then, the microcontroller begins filtering the Hall signals. An example of the acceleration and speed profile for this process is shown in Fig. 2-8. The output of filters (7) or (8) has a unit of time. Normalizing the filter output by the angular velocity ω_o at which the measurement is taken, a corresponding correction angle can be determined as

$$\Delta\phi^{corr} = \tau^{corr}\omega_o . \tag{2.9}$$

where $\Delta\phi^{corr}$ is the correction angle, τ^{corr} is the filter output time interval, and ω_o is the steady state electrical speed. These correction angles are then recorded into the LUT for future use and any other speeds and operating conditions of the given motor. Table 2-2 shows a fragment of such a LUT. There are six entries in this LUT corresponding to the six Hall states.

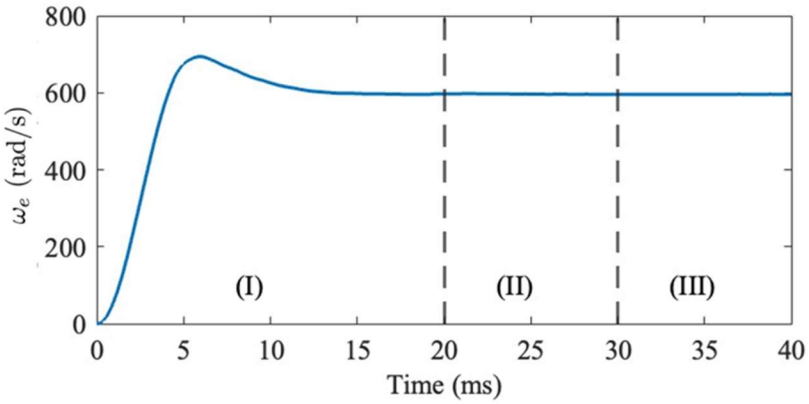

Figure 2-8 Speed profile of the calibration process. For segment (I), the motor reaches a steady state with original Hall signals. For segment (II), a filter is applied. For segment (III), the lookup table replaces the filter once the correction values are learned.

Since the LUT values are determined through a calibration routine, using the most accurate filter without the concern of delay would be advantageous for this stage. Therefore, higher-order filters, such as a six-step averaging filter, are preferred.

Table 2-2 A lookup table to balance conduction intervals.

Hall State	$\Delta\phi^{corr}$
1	$\Delta\phi_1^{corr}$
2	$\Delta\phi_2^{corr}$
3	$\Delta\phi_3^{corr}$
…	..

2.3.2. Reconstructed operation using LUT

During the reconstructed operation, the motor will use the correction angle values from the LUT to balance the conduction intervals. For each value in the LUT, the time between transitions will be

$$\tau_{LUT}^{corr} = \frac{\Delta\phi^{corr}}{\omega_e}. \tag{2.10}$$

Using this scheme, the reconstructed operation using the LUT successfully matched the performance of the six-step averaging filter methods for steady-state operation, as seen in Fig. 2-6. See Fig. 2-8 for the speed response during the calibration process.

2.4 Dynamic Performance

Previous research shows that the delay caused by the filters causes a negative impact on dynamics during fast acceleration [10]. Three primary transient behaviours were studied. These include a voltage-step transient, load-step transient, and startup transient.

2.4.1. Voltage-step transient

To emulate a voltage-step transient, the DC voltage of the VSI was stepped from 20V to 35V. Fig. 2-9 shows the resulting transient speed response. As seen in Fig. 2-9 (a), the motor with ideal sensors has a smooth acceleration response. The motors with 3-step and 6-step averaging filters have a mismatching transient in torque in Fig. 2-9 (c), which results in shocking the acceleration transients in Fig. 2-9 (b). These results are expected and consistent with the previous observations in [10]. At the same time, the motor with the proposed LUT-based correction algorithm performs very smoothly and closely matches the response of the motor with ideal sensors.

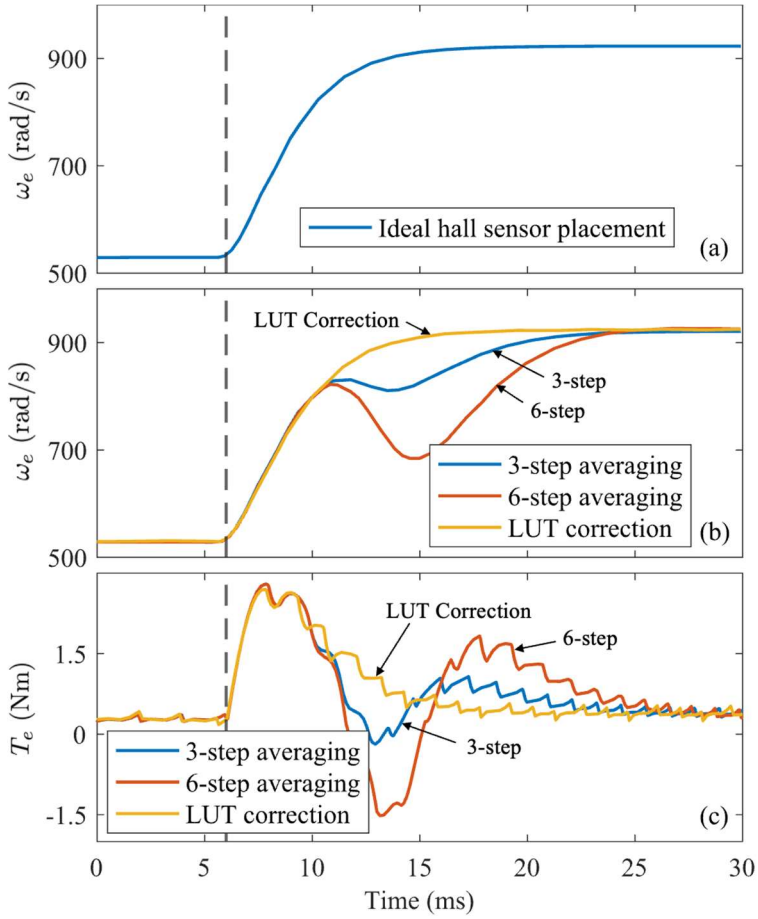

Figure 2-9 Simulated BLDC motor response to a DC voltage step increase: (a) the speed response of motor with ideal Hall sensor placement; (b) the speed response of motor with misaligned Hall sensors and corrected using filtering and proposed LUT correction; and (c) the electromagnetic torque response of motors with misaligned Hall sensors and corrected using filtering and proposed LUT correction.

2.4.2. Load-step transient

The mechanical load was stepped from 0.1 Nm to 1.0 Nm to simulate a load-step behaviour. The response in speed and electromagnetic torque is shown in Fig. 2-10. Notably, all considered correction methods perform reasonably well. This is because this deceleration transient is significantly slower ($6.2 \cdot 10^3$ rad/s^2) compared to the acceleration transient presented in Fig. 2-9 ($17.7 \cdot 10^3$ rad/s^2). At the same time, the proposed LUT-based correction method also has slightly

less oscillatory behaviour and reaches the final steady state speed a bit faster (compared to the averaging filter methods with some overshoots).

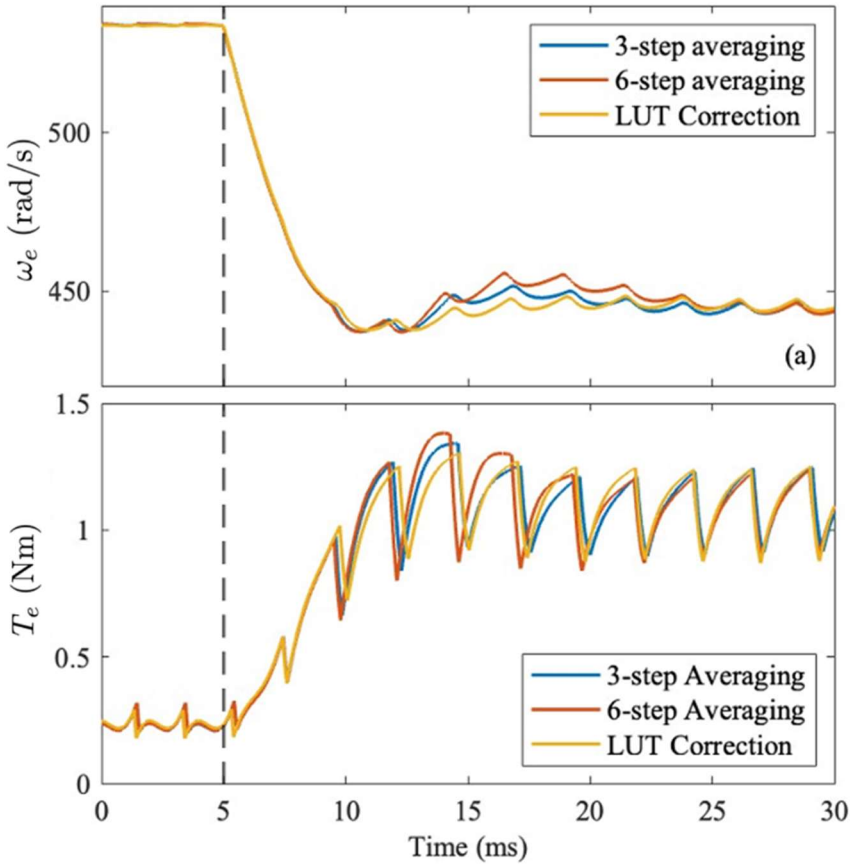

Figure 2-10 Simulated BLDC motors response to a load step increase using different mitigating control methods: (a) speed response, and (b) electromagnetic torque response. Three control methods are considered: 3-step and 6-step averaging filters and the proposed LUT-based correction algorithm.

2.4.3. Startup transient

Another drawback of the averaging filter-based methods [10] is that any filter with memory cannot start at zero speed and can only be activated after several switching intervals. In contrast, the proposed LUT-based correction method only depends on the current speed of the motor and the previously stored values in the LUT. Therefore, the proposed method can be activated after the first conduction interval. Fig. 2-11 shows the startup transient speed response of the BLDC motor

with the proposed LUT-based correction method. In this case, the LUT was turned on after about 4.5ms, and it demonstrates that this method can be used nearly from the start and without compromising the transient performance.

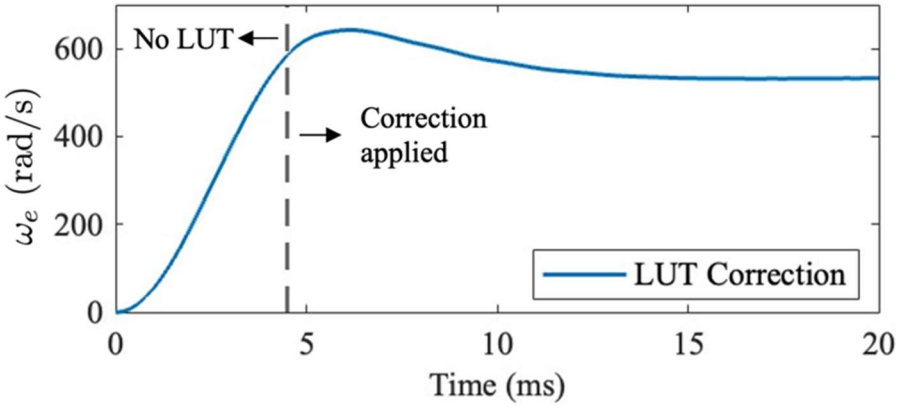

Figure 2-11 Speed response for startup transient when applying the LUT correction near the start of operation at the dashed line, one conduction interval after commencing.

2.5 Summary of simulation results

This chapter extended the previous work on improving the operation of widely used BLDC motors with the misalignment of Hall sensors. We proposed a two-stage method. The first stage uses a calibration routine and an averaging filter to identify the angle errors and record them into the LUT. In the second stage, the motor operates by reading out the correction angles and computing the corresponding correction times to balance conduction intervals and restore the motor operation. This leads to a new control method that works well in both steady-state fast transients and notably improves over previous methods. Simulation results were compared to measured values to ensure model correctness for steady-state operation. The following chapter will include a full digital implementation in an industrial/experimental BLDC motor controller.

Chapter 3: Microprocessor Implementation of a Lookup-Table-based Hall Sensor Correction Algorithm

Hall-sensor-controlled brushless DC (BLDC) motors are used in many applications due to their low cost, ease of control, and good torque/power characteristics. In an ideal case, the Hall sensors are spaced precisely 120 electrical degrees apart. However, in low-cost machines, there may be significant errors in the positioning of Hall sensors, leading to uneven conduction intervals and an increase in torque ripple. Previous research proposed averaging filters for balancing the Hall sensor signals and performance restoration. However, averaging filters also introduce a delay and may cause degradation of transient performance. This chapter showcases the implementation of the proposed mitigation algorithm on a microcontroller and results when demonstrated experimentally on a typical industrial BLDC motor, achieving significant improvement in transient performance over the previous methods.

3.1 Experimental Setup

Experiments are conducted on a typical industrial BLDC motor, such as the one illustrated in Fig. 2, whose parameters are summarized in the Appendix. The Hall-sensor misalignment was measured on three of such motors, and their errors are summarized in Table 3.1. As observed in Table I, the actual motors may have significant errors in Hall sensor signals when expressed in electrical degrees. Motor 1 was chosen as a good sample representing the phenomena of interest for the studies and experiments in this paper. The previous chapter included detailed modelling of Motor 1 and its verification in a steady state. The simulations were conducted in

MATLAB/Simulink using the Simscape Electrical Toolbox, and the system parameters were verified to achieve results that closely match the experimental measurements of phase currents and torque. This chapter is focused on implementing and demonstrating the proposed methodology on a microcontroller. The experimental setup is shown in Fig. 3-1, and it consists of a DC voltage supply connected to a voltage-source inverter, which controls the BLDC motor loaded by a DC machine dynamometer. The TI C2000^{TM} MCU series microcontroller is used here.

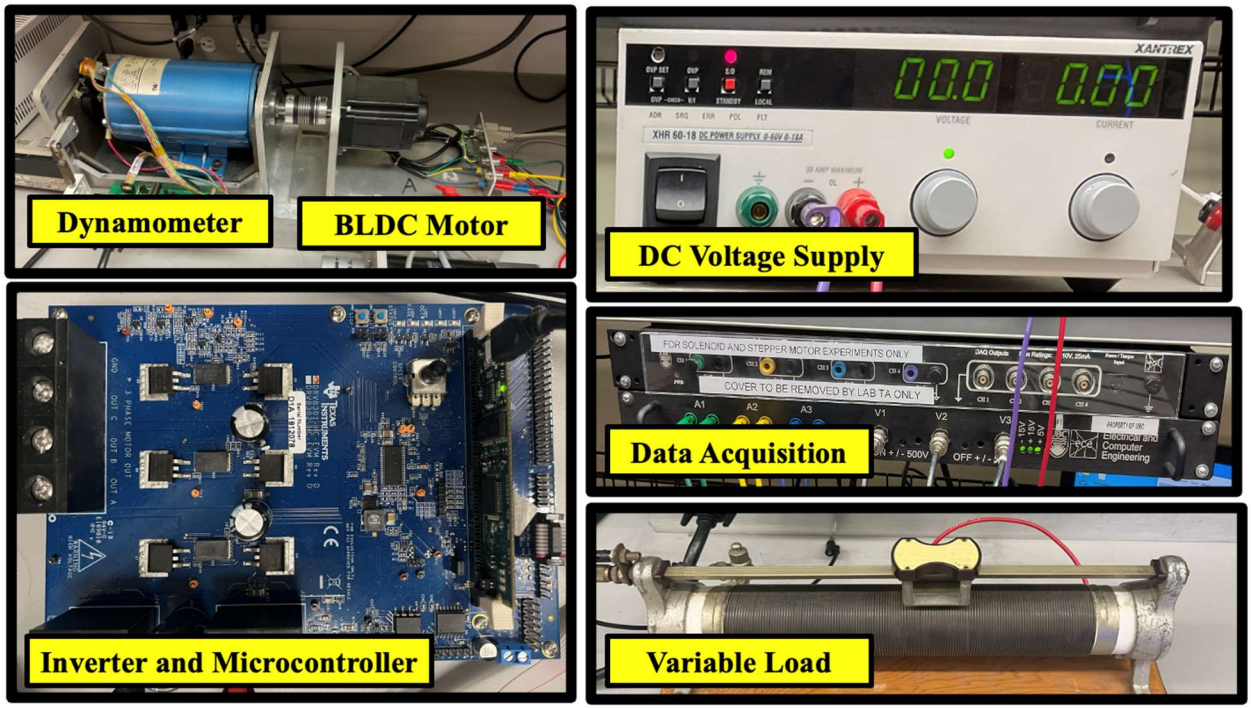

Figure 3-1 Experimental setup for measuring and controlling a BLDC motor.

Table 3-1 Hall-sensor misalignment in electrical degrees for three typical BLDC motors available in the lab. Motor 1 is used for experiments in this paper.

Motor Number	ϕ_A	ϕ_B	ϕ_C
1	9.0°	-1.0°	7.0°
2	5.0°	0.5°	-6.5°
3	2.0°	-3.5°	8.0°

3.1 Proposed Methodology

The correction algorithm proposed in chapter 2 was implemented on the TI C2000™ MCU series microcontroller. Fig. 3-2 shows the Control flow diagram for the lookup table-based algorithm. Initially, the algorithm uses an averaging filter to balance conduction intervals. Then, after a steady state is reached, the correction times from the averaging filter are converted into the correction angles and stored in a lookup table. The algorithm then switches to a second mode and starts using the correcting intervals from the lookup table instead of the averaging filter.

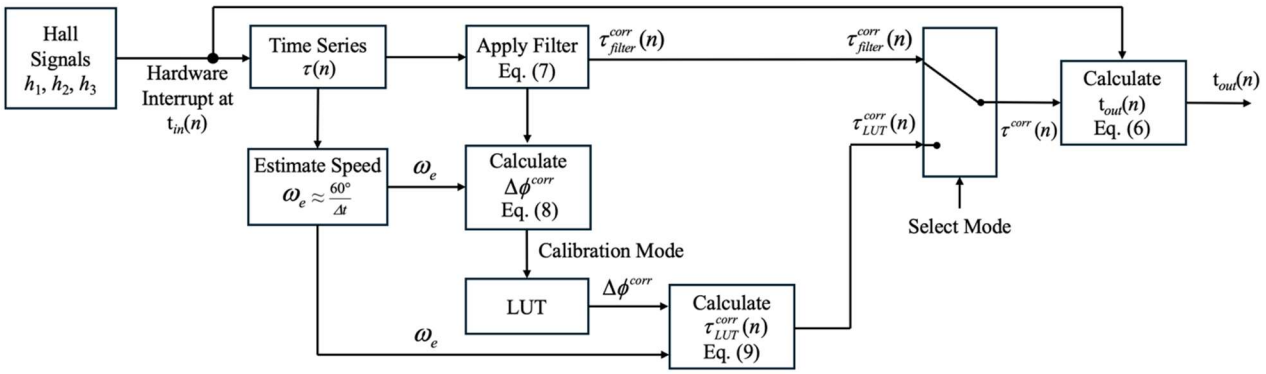

Figure 3-2 Control flow diagram for the correction algorithm.

The simulation work presented in [15] was validated by implementing this algorithm on a microcontroller, where conduction intervals were successfully balanced in steady-state (see Fig. 3-4). As observed in Fig. 3-4, the conduction intervals have become nearly balanced, where fluctuations between interval lengths dramatically decrease. Finally, Fig. 3-5 shows that the filter-based approach and LUT correction both produce very similar results in a steady state. After calibrating a motor, all subsequent operations can start with LUT operation, and re-calibration does not need to occur since Hall-sensor misalignment will not change over time. This gives this algorithm versatility, allowing the control algorithm to be calibrated without manual measurements, and thus, the calibration can easily be retaken if a system switches motors.

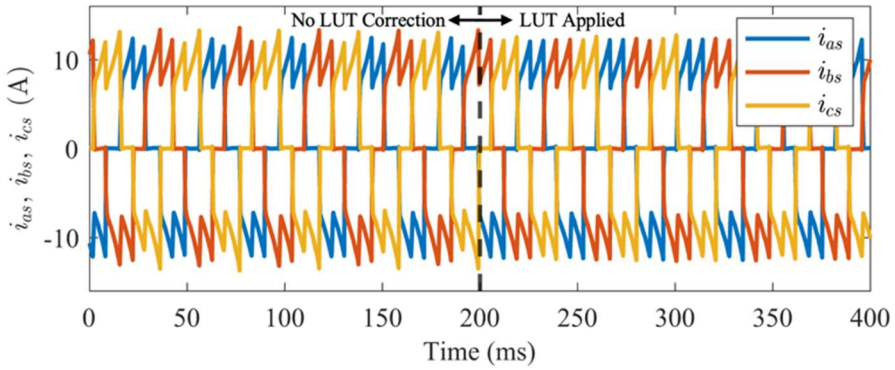

Figure 3-4 Applying a lookup table-based calibration successfully balanced conduction intervals.

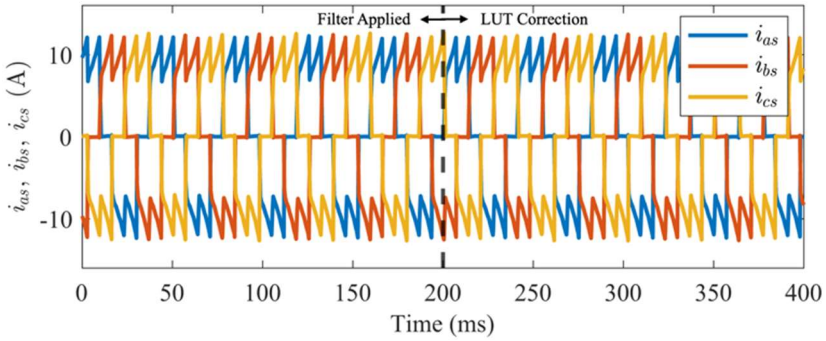

Figure 3-5 Transitioning from a filter-based approach to the lookup table correction method.

3.2 Dynamic Performance

Several transient studies have been conducted to demonstrate the dynamic performance of the proposed microcontroller-based methodology. Table 3-2 shows the lookup table for Motor 1 used throughout the studies in this chapter.

Table 3-2 Correction angles for Motor 1 identified in steady-state run time.

Hall State	$\Delta\phi^{corr}$
1	59.4°
2	62.5°
3	57.0°
4	55.7°
5	64.6°
6	60.4°

3.2.1. Startup transient

The proposed LUT-based correction scheme can be applied only after the appropriate correction terms have been obtained during a steady state and captured in the table. Fig.3-6 shows the startup transient recorded on the considered BLDC motor experimental setup. The conditions of this study were: a DC voltage of 24V, a duty cycle of 0.4, and a mechanical load set to 0.74Nm. In this case, the lookup table is already filled with pre-recorded values, and thus, the correction could be activated before reaching a steady-state.

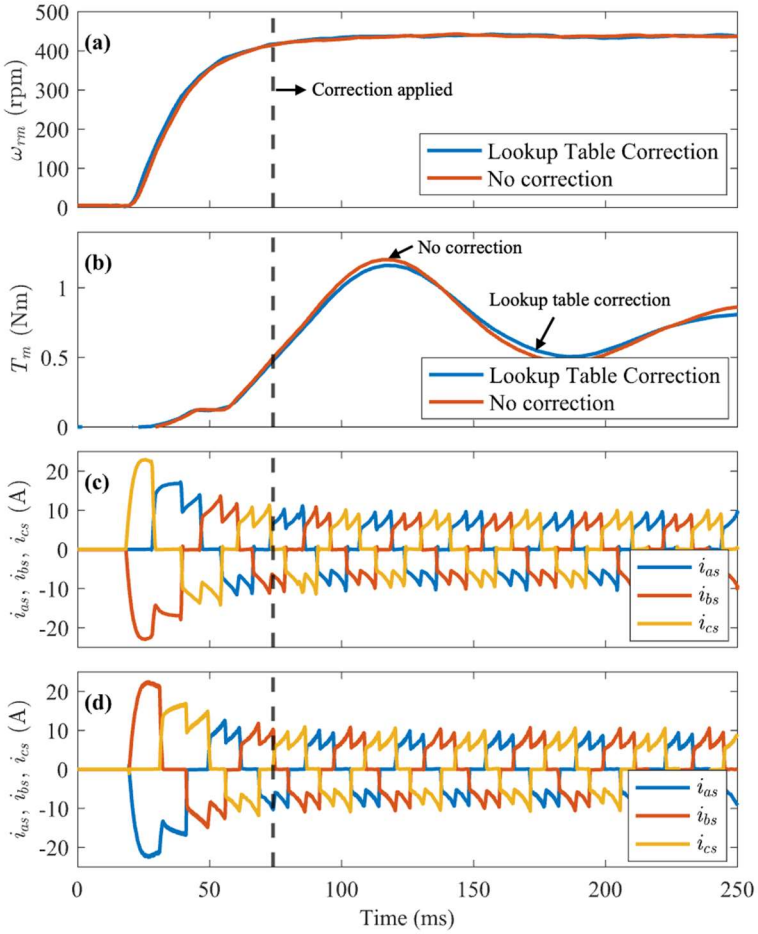

Figure 3-6 Measured startup transient as recorded by the DC dynamometer without and with the LUT correction: (a) speed response, (b) dynamometer reaction mechanical torque, (c) phase currents without LUT correction, and (d) phase currents with LUT correction.

The speed response is nearly identical to the uncorrected response, whereas the torque response is improved, leading to slightly less overshoot for the case using the lookup table. During the startup transient, the conduction intervals are balanced, leading to less current ripple for the phase currents with corrected Hall signals.

3.2.2 Voltage-step transient

To test a voltage-step transient, the duty cycle of the PWM was abruptly stepped from 0.2 to 0.6, causing the average DC voltage to step from 4.8V to 14.4V. Fig. 3-7 showcases the result of this transition. The speed profile for the 6-step averaging filter is significantly delayed, while the lookup table-based calibration method has a smooth profile, increasing monotonically until reaching a steady state. Additionally, the electromagnetic torque has a longer settling time for the 6-step averaging filter compared to the lookup table-based approach. During this study, the lookup table does not balance the Hall signals as cleanly as the 6-step averaging filter. This is because the speed must be estimated using just the previous conduction interval for fast speed estimation during transient behaviour. Future investigations could introduce a dynamic algorithm that adjusts the speed estimation depending on whether the operation is transient or steady-state.

3.4 Summary of Hardware Results

To conclude, this chapter provides hardware validation for the simulation-based chapter that introduces a novel calibration routine, exploring the possibility of correcting Hall-sensor misalignment by using a calibration routine using a lookup table. The goal of this new method was to balance uneven conduction intervals caused by the misalignment while eliminating the delay introduced by alternate correction methods such as a filter [6]. Through this chapter, the lookup table correction scheme was shown to be effective on a practical microprocessor, the TI C2000™

MCU series, commonly used in industry for motor control applications [16]. In particular, the new calibration routine improved the motor's transient performance, allowing voltage-step transients to take place without impacting performance.

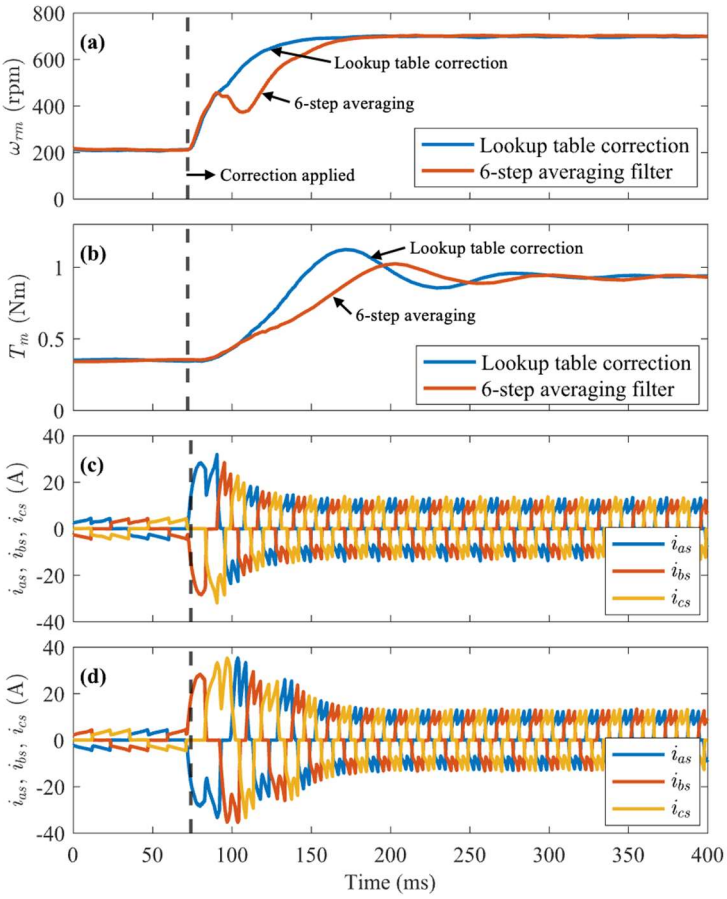

Figure 3-7 Measured response to a step change in the PWM duty cycle from 0.2 to 0.6 with the LUT and 6-step averaging correction: (a) speed response, (b) dynamometer reaction mechanical torque, (c) phase currents with LUT correction, and (d) phase currents with 6-step averaging filter correction.

Chapter 4: Conclusion

This thesis proposes a novel correction algorithm for brushless DC (BLDC) motors with misaligned Hall sensors, offering a significant contribution to low-cost BLDC machines. The proposed method builds upon a previously introduced filtering technique. The method works through a calibration routine by first allowing the machine to reach steady-state operation; in steady-state conditions, filter outputs are converted into conduction interval angles and tabulated into a lookup table. The motor then switches to a mode where conduction intervals are balanced through the lookup table. This method successfully improved upon the previous filter-based techniques by correcting Hall signals without introducing delay caused by high-order averaging filters.

The first section demonstrated the new proposed control algorithm in simulation, showing improvement in transient behaviour compared to previous mitigation techniques. Then, methods were further validated experimentally on a typical BLDC machine, the Arrow Precision Motor, where dynamic behaviour successfully matched simulation results. Future investigation into Hall-sensor misalignment should research combining this proposed technique with other advanced control schemes such as maximum torque per Ampere (MTPA) or maximum torque per Volt (MTPV).

3 Bibliography

[1] D. Mohanraj *et al.*, "A review of BLDC motor: state of art, advanced control techniques, and applications," *IEEE Access*, vol. 10, pp. 54833-54869, May 2022.

[2] P. Pillay and R. Krishnan, "Modeling, simulation, and analysis of permanent-magnet motor drives. I. The permanent-magnet synchronous motor drive," *IEEE Transactions on Industry Applications*, vol. 25, no. 2, pp. 265–273, 1989, doi: 10.1109/28.25541.

[3] R. Faturrohman, N. Ismail, and M. R. Effendi, "Speed Control System of BLDC Motor Based on DSP TMS320F28027F," pp. 1–5, Oct. 2022, doi: 10.1109/tssa56819.2022.10063899.

[4] R. Kumar, P. Kumar, B. Kumar, P. Singh, R. Kumar, and A. Kumar, "Design and Analysis of High Performance of a BLDC Motor for Electric Vehicle," *2022 2nd International Conference on Emerging Frontiers in Electrical and Electronic Technologies (ICEFEET)*, Jun. 2022, doi: 10.1109/icefeet51821.2022.9848307.

[5] M. Akrami, E. Jamshidpour, B. Nahid-Mobarakeh, S. Pierfederici, and V. Frick, "Sensorless Control Methods for BLDC Motor Drives: A Review," *IEEE Transactions on Transportation Electrification*, pp. 1–1, Jan. 2024, doi: 10.1109/tte.2024.3387371.

[6] N. Samoylenko, Q. Han, and J. Jatskevich, "Dynamic Performance of Brushless DC Motors With Unbalanced Hall Sensors," *IEEE Transactions on Energy Conversion*, vol. 23, no. 3, pp. 752–763, Sep. 2008, doi: 10.1109/tec.2008.921555.

[7] P. Alaeinovin and J. Jatskevich, "Filtering of Hall-Sensor Signals for Improved Operation of Brushless DC Motors," *IEEE Transactions on Energy Conversion*, vol. 27, no. 2, pp. 547–549, Jan. 2012, doi: 10.1109/tec.2011.2180171.

[8] P. C. Krause, O. Wasynczuk, S. D. Pekarek, and T. O'Connell, "Electromechanical Motion Devices: Rotating Magnetic Field-based Analysis with Online Animations," Hoboken: John Wiley & Sons, 2020.

[9] S. D. Sudhoff and P. C. Krause, "Operating modes of the brushless DC motor with a 120 degrees inverter," *IEEE Transactions on Energy Conversion*, vol. 5, no. 3, pp. 558–564, 1990, doi: 10.1109/60.105282.

[10] P. Alaeinovin, S. Chiniforoosh, and J. Jatskevich, "Evaluating misalignment of hall sensors in brushless DC motors," *IEEE Canada Electric Power Conference*, Oct. 2008, doi: 10.1109/epc.2008.4763350.

[11] N. Samoylenko, Q. Han, and J. Jatskevich, "Improving Dynamic Performance of Low-Precision Brushless DC Motors with Unbalanced Hall Sensors," *IEEE Power Engineering Society General Meeting*, Jun. 2007, doi: 10.1109/pes.2007.386221.

[12] J. S. Park, J.-H. Choi, and J. Lee, "Compensation Method of Position Signal Error with Misaligned Hall-Effect Sensors of BLDC Motor," *Journal of Electrical Engineering and Technology*, vol. 11, no. 4, pp. 889–897, Jul. 2016, doi: 10.5370/jeet.2016.11.4.889.

[13] P. L. Chapman, S. D. Sudhoff, and C. A. Whitcomb, "Multiple reference frame analysis of non-sinusoidal brushless DC drives," *IEEE Transactions on Energy Conversion*, vol. 14, no. 3, pp. 440–446, Sep. 1999, doi: 10.1109/60.790894.

[14] J. Zhou, "Maximum torque per Ampere and maximum torque per voltage operation of brushless DC motor drive systems with extended switching schemes," M.S. thesis, University of British Columbia, Vancouver, Canada, 2022.

[15] M. Hasman, M. Phung, Z. Feng and J. Jatskevich, "Mitigating Misaligned Hall-Sensors in Brushless DC Motors Using Calibration Routine," 2025 24th International Symposium

INFOTEH-JAHORINA (INFOTEH), East Sarajevo, Bosnia and Herzegovina, 2025, pp. 1-7, doi: 10.1109/INFOTEH64129.2025.10959174.

[16] D. F. Ramirez Jimenez, A. L. Parrado and J. V. Medina, "Overview of a framework for Implementation of digital controllers in Energia IDE using Texas Instruments microcontrollers," *2021 IEEE 5th Colombian Conference on Automatic Control (CCAC)*, Ibague, Colombia, 2021, pp. 13-18, doi: 10.1109/CCAC51819.2021.9633305.

Statement on the Use of AI:

The research presented in this thesis was conducted without relying on AI tools. All of the text, images, captions, and data were made without the use of AI.

Appendix A - Parameters of Experimental Setup

BLDC machine parameters: Arrow Precision Motor Company, Ltd., Model 86EMB3S98F, 8 poles, $r_s = 0.15\Omega$, $L_{ss} = 0.45$ mH, $\lambda'_m = 21.5$mV·s, and $J_{total} = 1.2 \cdot 10^{-4}$ Nm·s^2.

Microcontroller and voltage-source inverter: DRV8301-HC-EVM VSI development board with TI F28035 control card (TI C2000^{TM} MCU series).